Miscible displacements in capillary tubes: Influence of Korteweg stresses and divergence effects

Ching-Yao Chen[a)]
Department of Mechanical Engineering, Da-Yeh University, Chang-Hua, Taiwan 515, Republic of China

Eckart Meiburg
Department of Mechanical and Environmental Engineering, University of California at Santa Barbara, Santa Barbara, California 93106

(Received 16 October 2001; accepted 4 April 2002; published 17 May 2002)

The question is addressed as to whether Korteweg stresses and/or divergence effects can potentially account for discrepancies observed between conventional Stokes flow simulations (Chen and Meiburg) and experiments (Petitjeans and Maxworthy) for miscible flows in capillary tubes. An estimate of the vorticity and stream function fields induced by the Korteweg stresses is presented, which shows these stresses to result in the formation of a vortex ring structure near the tip of the concentration front. Through this mechanism the propagation velocity of the concentration front is reduced, in agreement with the experimental observations. Divergence effects, on the other hand, are seen to be very small, and they have a negligible influence on the tip velocity. As a result, we can conclude that they are not responsible for the discrepancies between experiments and conventional Stokes simulations. © *2002 American Institute of Physics.* [DOI: 10.1063/1.1481507]

I. INTRODUCTION

Displacements in capillary tubes have long served as paradigm flows for the investigation of mechanisms governing two-phase flows. In the immiscible case the studies by Taylor[3] and Cox,[4] as well as the corresponding calculations by Reinelt and Saffman,[5] represent classical examples, cf. also the fundamental theoretical investigation by Bretherton[6] for long bubbles. Taylor measures the amount of fluid displaced by injecting air into a horizontal capillary tube, initially filled with a viscous fluid, in order to calculate the thickness of the film of displaced fluid left behind on the wall of the tube as a function of the capillary number Ca. However, in Taylor's experiment the flow in the interior of the finger is dynamically unimportant because of the large viscosity ratios. The numerical simulations by Reinelt and Saffman,[5] based on the Stokes equations, agree very closely with these experiments. Unfortunately, no comparable experiments have been conducted for finite viscosity ratios.

Petitjeans and Maxworthy[2] as well as Chen and Meiburg[1] carry out a corresponding collaborative investigation for miscible fluids. In these flows, a cutoff length is set by diffusive effects rather than surface tension, so that in some sense the Péclet number Pe takes the place of Ca. These authors also address finite viscosity ratios by varying the Atwood number At, as well as the role of density differences (expressed by a further dimensionless parameter F) by conducting experiments and simulations in vertical tubes. The miscible and immiscible cases differ fundamentally in that the miscible flow can never become truly steady. Sooner or later, diffusion will cut off the supply of fresh displacing fluid, and for long times the case of Poiseuille flow and Taylor dispersion (Taylor[7]) will be approached. Nevertheless, both simulations and experiments show that for large values of Pe, typically above $O(10^3-10^4)$, a quasisteady finger forms. In this parameter regime, the experimentally and numerically observed amount of displaced fluid left behind on the tube walls for $\mathrm{At}\rightarrow 1$ matches Taylor's[3] immiscible data. On the other hand, the largest discrepancy between the experiments of Petitjeans and Maxworthy[2] and the Stokes simulations of Chen and Meiburg[1] is observed at small values of Pe, in that a quasisteady finger emerges for significantly smaller values of Pe in the simulations, as compared to the experiments. At these low Pe values, the experimentally observed diffusive front between the injected, less viscous fluid, and the resident more viscous phase hence appears to be less prone to the strong deformation needed to form a finger, as compared to the numerically simulated flow based on the conventional Stokes equations. The present, computational investigation takes a step towards identifying the reasons behind this discrepancy by addressing the influence of various physical mechanisms not contained in the standard set of Stokes equations.

In miscible flows involving fluids of different densities, phenomena are present that frequently are not accounted for in theoretical or computational analyses. Even if the two fluids are incompressible, the usual mass-averaged velocity is not divergence free in the mixing region, cf. Hu and Joseph.[8] However, numerical simulations of such fluid flows routinely assume this effect to be small (without providing a quantitative estimate for its size), and employ a solenoidal velocity field. It is hence important to establish the range of validity of this approach. In addition, as discussed by Davis,[9] Hu and Joseph,[8] Joseph and Renardy,[10] and Chen, Wang, and Meiburg,[11] additional so-called Korteweg stresses

[a)]Author to whom all correspondence should be addressed. Electronic mail: chingyao@mail.dyu.edu.tw

(Korteweg[12]) can potentially be important in regions of large concentration gradients. While a first principles derivation, or even a detailed model, for the action of such stresses is not yet available, there exist proposals in the literature for their mathematical formulation, cf. Galdi *et al.*,[13] Joseph and Renardy,[10] and Joseph *et al.*[14] However, the magnitude of the coefficients in the expressions for these stresses is presently unknown. Interestingly, there exists information regarding the sign of the Korteweg stress constant based on the work by Hu and Joseph,[8] who point out that in miscible Hele-Shaw flows this constant has to be negative in order to avoid Hadamard instability, or mathematical ill posedness of the problem. This represents important information, as it allows us to determine if the action of the postulated Korteweg stresses points in the right direction in order to possibly account for discrepancies between experiments and numerical simulations that do not consider these stresses. Scaling arguments regarding the magnitude of the stresses are provided by Davis,[9] while Petitjeans and Maxworthy[2] arrive at an estimate of 5×10^{-4} N/m, based on a comparison with the immiscible observations by Taylor.[3] Further efforts in this direction have been undertaken by Petitjeans and coauthors (Petitjeans,[15] Petitjeans and Kurowski,[16] Kurowski and Misbah[17]).

Due to the present lack of detailed experimental measurements, the current investigation represents a first, somewhat qualitative step intended to shed light on the nature and potential magnitude of the above effects in miscible capillary flows. The goal is to obtain information as to whether Korteweg stresses and divergence effects modify the pure Stokes flow results in a direction consistent with the observed experimental/numerical discrepancies alluded to above. In this context, it should be pointed out that cylindrical tubes represent only one of the fundamental geometries. Another one of great practical importance is the plane, narrow gap between two plates, i.e., the classical Hele-Shaw configuration, cf. the review by Homsy.[18] Here many of the same phenomena arise, but in addition there is the issue of the length scale selection in the spanwise direction, or in the circumferential direction for the case of a localized injection. A recent comparison between experiments of the density driven instability between miscible fluids in a vertically arranged Hele-Shaw cell (Fernandez *et al.*[19]) and a corresponding linear stability analysis based on the three-dimensional Stokes equations (Graf, Meiburg, and Härtel[20]) shows systematic discrepancies for low values of the Rayleigh number Ra that may have their origin in similar physical phenomena as the above mentioned low Pe differences.

II. PHYSICAL PROBLEM AND GOVERNING EQUATIONS

The present computational investigation focuses on the temporal evolution of axisymmetric miscible interfaces in horizontal and vertical capillary tubes. Our goal is to compare with the experiments of Petitjeans and Maxworthy,[2] in which the Reynolds number is small and inertial terms are negligible. According to Joseph and Renardy[10] as well as Joseph *et al.*,[14] under these circumstances the governing equations expressing the balance of mass, momentum and species for simple binary mixtures in a vertical capillary tube take the form

$$\frac{\partial c}{\partial t}+\nabla\cdot(\mathbf{u}c)=\nabla\cdot\left(\frac{D}{1-\xi c}\nabla c\right), \tag{1}$$

$$\nabla\cdot\left(\mathbf{u}-\frac{\xi D}{1-\xi c}\nabla c\right)=0, \tag{2}$$

$$\nabla(P+Q(c))=\nabla\cdot(2\mu D[\mathbf{u}]+\delta_1(\nabla c)(\nabla c)^T)+\rho\mathbf{g}. \tag{3}$$

Here, $\mathbf{u}$ denotes the conventional, mass-averaged velocity, c the concentration of the lighter fluid, ξ the normalized density difference, D the constant diffusion coefficient, and p the pressure. The viscosity is indicated by μ, while Q represents an additional pressure component due to Korteweg stresses, as explained by Joseph.[21] δ_1 denotes the coefficient of the Korteweg stresses related to concentration gradients in the flow.

In order to render the governing equations dimensionless, we take the tube diameter d as the characteristic length scale and define a characteristic time scale as $\mu_h/gd\Delta\rho$. Here μ_h indicates the viscosity of the heavier fluid, and $\Delta\rho$ represents the density difference driving the instability. Following standard assumptions employed in the literature on miscible porous media flows, we employ viscosity-concentration and density-concentration relationships of the form

$$\mu(c)=e^{Rc}, \tag{4}$$

$$\rho(c)=\frac{\rho_h}{\Delta\rho}-c. \tag{5}$$

This type of dependence on the concentration is commonly assumed in the literature on miscible fluids, and it closely approximates the behavior of the fluids used in the experiments of Petitjeans and Maxworthy.[2] By introducing the solenoidal volume averaged velocity $\mathbf{W}$,

$$\mathbf{W}=\mathbf{u}-\frac{\xi D}{1-\xi c}\nabla c, \tag{6}$$

$$W_z=\frac{1}{r}\frac{\partial\psi}{\partial r},\quad W_r=-\frac{1}{r}\frac{\partial\psi}{\partial z}, \tag{7}$$

we can reformulate the governing equations in terms of a stream function

$$\nabla^4\psi=G(R,z,r,\psi,c)-\frac{2r\xi}{\mathrm{Pe}}f(R,z,r,c)$$
$$-\frac{r\delta}{\mu}h(R,z,r,c)-\frac{r}{\mu}\frac{\partial c}{\partial r}, \tag{8}$$

$$\frac{\partial c}{\partial t}+\mathbf{W}\cdot\nabla c=\frac{1}{\mathrm{Pe}}\nabla^2 c, \tag{9}$$

where the Peclet number Pe and dimensionless Korteweg constant δ take the forms

$$\mathrm{Pe}=\frac{gd^3\Delta\rho}{\mu_h D},\quad \delta=\frac{\delta_1}{gd^3\Delta\rho}. \tag{10}$$

Here the function G indicates the viscous terms, cf. Chen and Meiburg,[1] and the last term on the right-hand side accounts for gravitational effects, while f and h capture the effects of divergence and the Korteweg stresses, respectively,

$$f=-\frac{2}{r^2}\frac{\partial^2 c}{\partial r\partial z}+R\left\{\frac{1}{r}\frac{\partial^2 c}{\partial r\partial z}\frac{\partial c}{\partial r}-\frac{1}{r}\frac{\partial^2 c}{\partial r^2}\frac{\partial c}{\partial z}+\frac{\partial^3 c}{\partial r^2\partial z}\frac{\partial c}{\partial r}+\frac{\partial^3 c}{\partial z^3}\frac{\partial c}{\partial r}-\frac{\partial^3 c}{\partial z^2\partial r}\frac{\partial c}{\partial z}-\frac{\partial^3 c}{\partial r^3}\frac{\partial c}{\partial z}\right\}+R^2\left\{\left(\frac{\partial c}{\partial r}\right)^2\frac{\partial^2 c}{\partial r\partial z}+\frac{\partial^3 c}{\partial z^3}\frac{\partial c}{\partial r}-\frac{\partial^3 c}{\partial z^2\partial r}\frac{\partial c}{\partial z}-\frac{\partial^3 c}{\partial r^3}\frac{\partial c}{\partial z}\right\},$$

$$h=\frac{1}{r}\frac{\partial^2 c}{\partial r^2}\frac{\partial c}{\partial z}-\frac{1}{r}\frac{\partial^2 c}{\partial r\partial z}\frac{\partial c}{\partial r}-\frac{2}{r^2}\frac{\partial c}{\partial z}\frac{\partial c}{\partial r}+\frac{\partial^3 c}{\partial r^3}\frac{\partial c}{\partial z}-\frac{\partial^3 c}{\partial r^2\partial z}\frac{\partial c}{\partial r}+\frac{\partial^3 c}{\partial z^2\partial r}\frac{\partial c}{\partial z}-\frac{\partial^3 c}{\partial z^3}\frac{\partial c}{\partial r}.$$

In the derivation of Eq. (8) we have assumed $\xi/(1-\xi c)\approx\xi$. In this way ξ effects are considered only to leading order in the momentum balance. This assumption is in close agreement with the experiments of Petitjeans and Maxworthy,[2] in which $\xi<0.1$. By employing the above stream-function-based formulation, the appearance of the additional pressure term Q in Eq. (3) is eliminated. Boundary conditions are prescribed as

$$z=z_1,z_2:\quad \frac{\partial^2 c}{\partial z^2}=0,\quad \frac{\partial^2\psi}{\partial z^2}=0,\quad \frac{\partial^4\psi}{\partial z^4}=0, \tag{11}$$

$$r=0:\quad \frac{\partial c}{\partial r}=0,\quad \psi=0,\quad \frac{\partial\psi}{\partial r}=0, \tag{12}$$

$$r=0.5:\quad \frac{\partial c}{\partial r}=0,\quad \psi=0,\quad \frac{\partial\psi}{\partial r}=-\frac{\xi}{2\mathrm{Pe}}\frac{\partial c}{\partial z}. \tag{13}$$

The stream-function equation is solved by means of a multigrid technique based on second order central differencing discretization. An ADI scheme (Fletcher[22]) in conjunction with third order upwind differencing is used to advance the concentration equation in time.

III. RESULTS

A. Miscible displacement in a horizontal capillary tube

Before focussing on the unstably stratified flow in a vertical capillary tube, we will address the related situation analyzed by Petitjeans and Maxworthy,[2] as well as Chen and Meiburg.[1] Here a less viscous fluid is injected into a horizontal capillary tube initially filled with a more viscous one, i.e., a net flow rate is present. If the cross section of the tube is small, gravitational effects do not affect the flow in a significant way and can be neglected. The fluids are again fully miscible, and a suitable Péclet number is now defined as

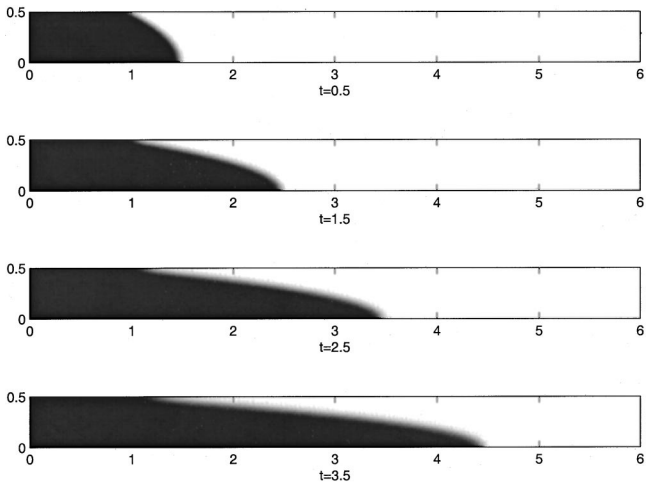

FIG. 1. Temporal evolution of a passive concentration field in axisymmetric Poiseuille flow for Pe=2000 at times $t=0.5$, 1.5, 2.5, and 3.5.

$$\mathrm{Pe}=\frac{Ud}{D}, \tag{14}$$

where U is the center line velocity of the Poiseuille flow with the same volumetric flow rate. For sufficiently large values of Pe, the less viscous fluid is seen to propagate along the center line, while a film of the resident fluid is left behind on the tube wall. The thickness of this film depends on Pe, as well as on the viscosity ratio of the two fluids. Numerical simulations based on the Stokes equations showed close agreement with the experiments for large values of Pe. However, for small Peclet numbers a clear discrepancy was observed, in that the simulations showed the emergence of quasisteady fingers for $\mathrm{Pe}>O(10^3)$, whereas in the experiments such fingers did not appear until $\mathrm{Pe}\sim O(10^4)$. The question then arises as to whether Korteweg-type stresses, which were not accounted for in the simulations, may be responsible for delaying the appearance of the quasisteady fingers in the experiments.

In order to address the question as to whether the action of the Korteweg stresses points in the right direction in order to account for the observed difference between experiments and simulations, we numerically tracked the spatiotemporal evolution of a *passive* concentration field under the action of diffusion in an axisymmetric Poiseuille flow. Initially, the concentration field is uniform across the tube diameter and has a steep, error function-like profile in the axial direction. This is the classical case of Taylor dispersion (Taylor[7]). For a Pe value of 2000, the concentration field at different times is shown in Fig. 1. Its overall features are similar to the concentration field that would emerge in a variable viscosity flow, cf. Chen and Meiburg.[1] Consequently, it is well suited for evaluating qualitatively the nature of the effects that Korteweg stresses would have in such a flow, if they were taken into account. To this end, we calculate the Korteweg stresses from the concentration field shown in Fig. 1, up to the unknown coefficient that multiplies the Korteweg stress term in Eq. (8). We subsequently solve the equation

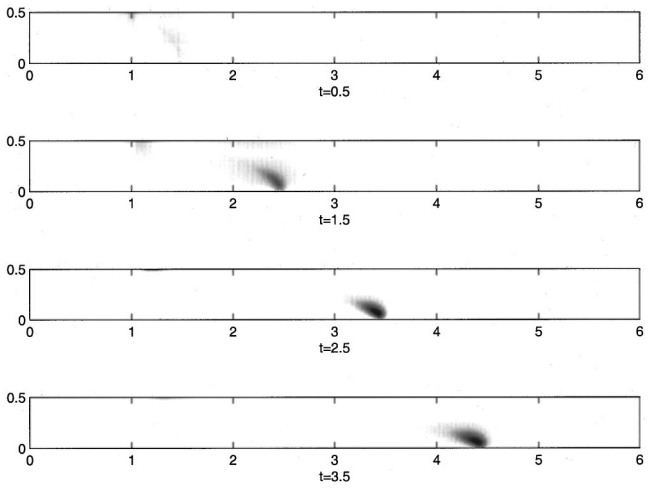

FIG. 2. Vorticity distribution that would be generated as a result of the Korteweg stresses by the concentration fields shown in Fig. 1. The vorticity field is determined up to a constant factor, which is related to the unknown Korteweg stress coefficient.

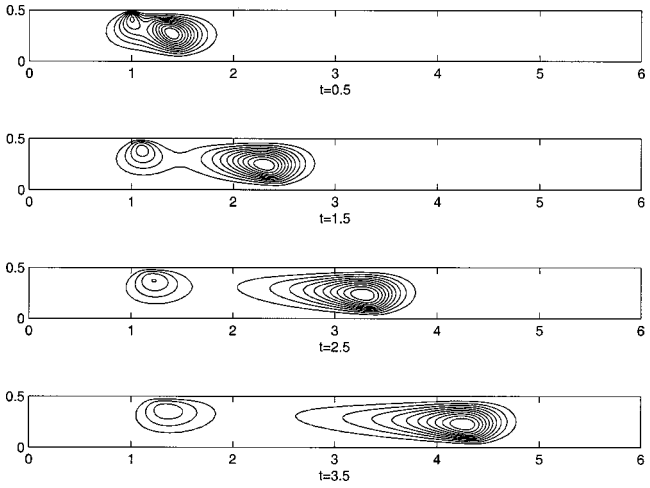

FIG. 3. Stream-function distribution corresponding to the vorticity fields shown in Fig. 2. A ring-like vortex structure is seen to emerge at the tip of the concentration front. For negative Korteweg stress coefficients, as postulated by Hu and Joseph (Ref. 8), this vortex ring causes an upstream velocity at the center line of the tube, thereby slowing the front down and stabilizing it.

$$\nabla^4\psi \equiv -\nabla^2\omega = -\frac{r\delta}{\mu}h(R,z,r,c), \tag{15}$$

in order to obtain the distribution of the vorticity and stream-function fields that these stresses would generate if they were taken into account. This information is presented in Figs. 2 and 3. The formation of a ring-like vortex near the tip of the concentration front is clearly visible. If the unknown coefficient δ has a negative value, as postulated by Hu and Joseph,[8] the vorticity in this ring is oriented such that the flow is retarded near the axis, while it is being accelerated near the tube wall. In this way, a negative δ value acts to slow the kind of frontal deformation that leads to the emergence of a finger propagating along the tube axis. This reflects the fact that at the tip of the front, the normal stress component is $\delta(\partial c/\partial z)^2$, which for negative values of δ always opposes the spreading of the front. Thus we find that the effect of the postulated Korteweg stresses on the present flow has the correct sign in order to potentially explain the discrepancy between the experiments of Petitjeans and Maxworthy[2] and the Stokes simulations of Chen and Meiburg.[1] However, when we included this Korteweg stress in the governing equations, we could never achieve the complete stabilization of the front that appears to take place in the experiments of Petitjeans and Maxworthy[2] at comparable Pe values, even if we employed Korteweg stress coefficients that were several orders of magnitude larger than available estimates in the literature. We plan to undertake a more detailed investigation, in order to resolve this discrepancy.

B. Unstable density stratification in a vertical capillary tube

In the following, the focus is on the temporal evolution of an axisymmetric miscible interface formed by placing a heavier and more viscous fluid above a lighter and less viscous one in a vertically oriented capillary tube. Preliminary results for this configuration were reported by Chen, Meiburg, and Wang.[23]

1. Flow behavior for different Peclet numbers and viscosity ratios

Figure 4 shows the temporal evolution of the flow for $\mathrm{Pe}=2\times10^5$ and $R=-2.5$, in the absence of divergence effects or Korteweg stresses. The interface is initially perturbed in such a fashion that it is slightly elevated in the center of the tube compared to near the tube walls. It should be pointed out that we are mostly interested in the asymptotic long-term features of the flow, which test calcu-

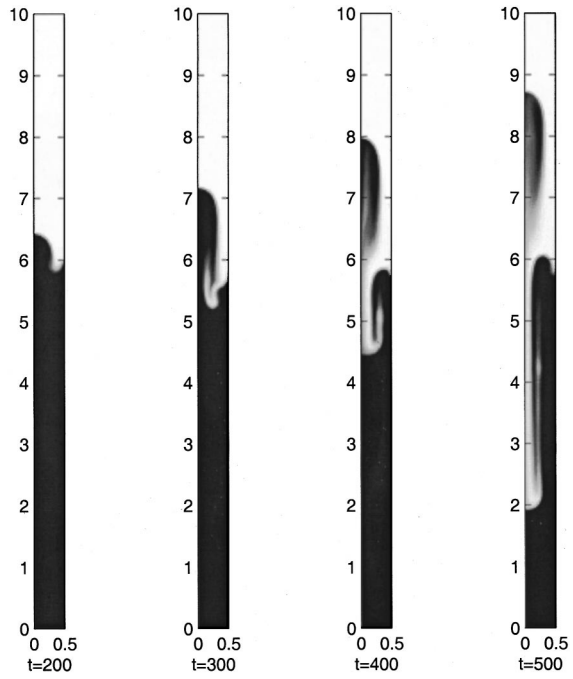

FIG. 4. Unstable evolution of the axisymmetric miscible interface formed by placing a heavier fluid above a lighter one, in the absence of Korteweg stresses and divergence effects. $\mathrm{Pe}=2\times10^5$ and $R=-2.5$. A bubble of the lighter fluid is seen to pinch off and rise at a nearly constant velocity.

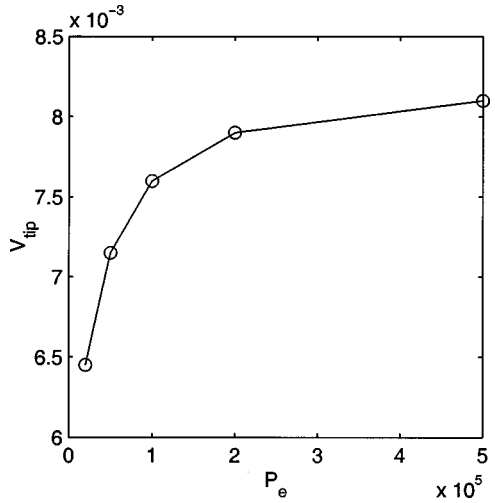

FIG. 5. The tip velocity V_{tip} as a function of Pe for $R=-2.5$, in the absence of Korteweg stresses and divergence effects. With increasing Pe, V_{tip} is seen to asymptotically approach a plateau.

lations showed to be independent of the precise form of the initial conditions. An instability is seen to develop, which leads to the rise of the lighter fluid along the tube axis, while the heavier fluid flows downwards at larger radii. Soon, however, the heavier fluid separates from the wall and forms a downward propagating finger along the axis of the tube. The bubble of lighter fluid thus formed pinches off and continues to rise along the tube center, while additional light fluid begins to rise near the outer walls. The bubble continues to rise in a quasisteady fashion with a nearly constant velocity. At the present viscosity ratio, a qualitatively similar evolution of the flow is observed over a large range of Pe, with numerically observed bubble rise velocities V_{tip} as shown in Fig. 5.

At larger viscosity ratios, an identical initial perturbation does not lead to the pinchoff of a rising bubble. Instead, the lighter fluid continues to rise along the tube center line, so that a well developed finger forms that remains connected to the body of lighter fluid in the lower portion of the tube, cf. the case of $R=-4.5$ shown in Fig. 6. Figure 7 shows the tip velocity V_{tip} as a function of the viscosity ratio for $\mathrm{Pe}=5\times10^4$. For infinite viscosity ratios it asymptotes towards a plateau that is close to the value of 0.0102 reported by Clift, Grace, and Weber[24] for the immiscible situation of a long air slug in a tube filled with water.

2. Influence of Korteweg stresses

In order to evaluate the effects of the postulated Korteweg stresses on the tip propagation velocity, we carried out simulations for various magnitudes of the dimensionless parameter δ. The range of δ was selected on the basis of the values provided by Davis.[9] In agreement with the findings of Hu and Joseph,[8] only negative values were employed. There are no divergence effects present in the flow, and the values of Pe and R are kept at 10^5 and -2.5, respectively. Figure 8 shows the tip velocity V_{tip} to decrease by as much as 10% as the Korteweg stresses grow in strength, which demonstrates their stabilizing effect.

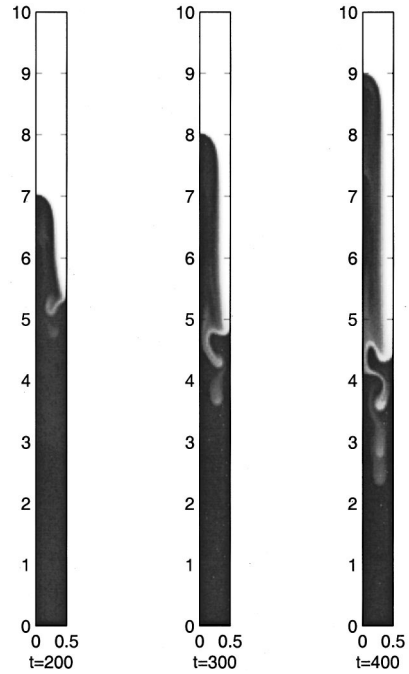

FIG. 6. Unstable evolution of the interface for $\mathrm{Pe}=5\times10^4$ and $R=-4.5$, in the absence of Korteweg stresses and divergence effects. For these flow parameters, a bubble does not form. Rather, a continuous finger of the lighter and less viscous fluid rises along the tube center line.

This stabilizing effect of the Korteweg stresses can be understood on the basis of the governing equations from the information provided in Fig. 9. Figures 9(a) and 9(b) show the concentration and stream-function distributions for $\mathrm{Pe}=10^5$ and $R=-2.5$ in the absence of Korteweg stresses. Figures 9(c) and 9(d) present the corresponding distributions in the presence of Korteweg stresses for a value of $\delta=-10^{-4}$. In addition, for this flow Fig. 9(e) displays the component of the stream function due to the Korteweg stresses only. Near the tip of the bubble, these stresses are

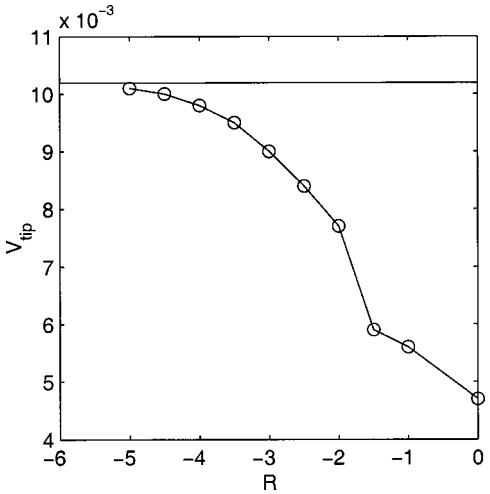

FIG. 7. Tip velocity vs viscosity ratio: Asymptotic values for large Pe, in the absence of Korteweg stresses and divergence effects. For large viscosity contrasts, the tip velocity asymptotically approaches a level that is close to the value of 0.0102 measured by Clift, Grace, and Weber (Ref. 24) for a long air bubble in a tube filled with water.

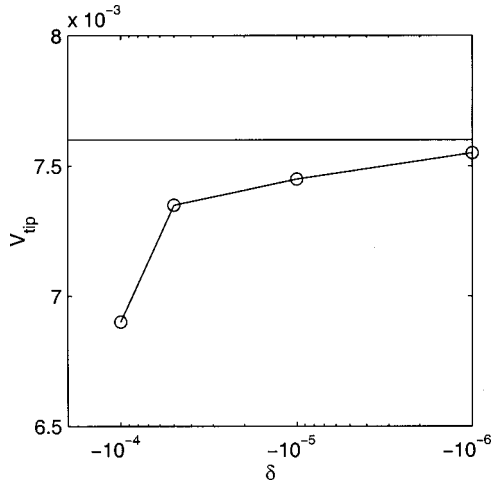

FIG. 8. Tip velocity vs Korteweg stress constant δ for $\mathrm{Pe}=10^5$ and $R=-2.5$, in the absence of divergence effects. In line with the findings of Hu and Joseph (Ref. 8), only negative values are considered for δ. The corresponding Korteweg stresses are seen to slow down the tip of the rising finger of lighter fluid. The horizontal line indicates the value obtained for $\delta=0$.

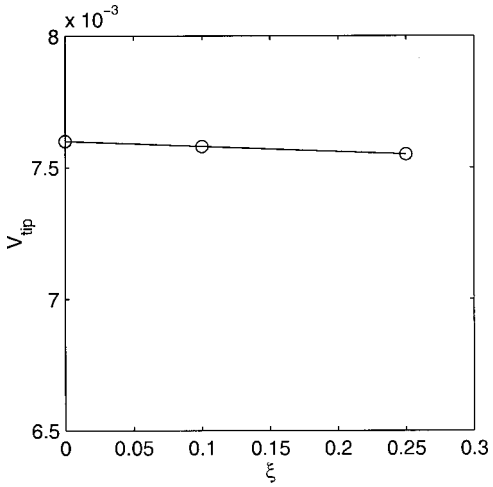

FIG. 10. Tip velocity vs divergence coefficient ξ for $\mathrm{Pe}=10^5$ and $R=-2.5$, in the absence of Korteweg stresses. Divergence effects are seen to have a negligible effect on the tip velocity, even for large values of ξ up to 0.25.

again seen to generate a ring-like vorticity distribution that induces a downward velocity on the tube axis, similar to the case of the horizontal tube discussed above. In this way, the Korteweg stresses slow down the rising bubble. Unlike for the case of the horizontal capillary tube discussed above, we do not at present have experimental data for the vertical tube to compare with. The availability of such experimental data might allow us to obtain estimates for the magnitude of the Korteweg stress coefficient, as the rise velocity shows the pronounced sensitivity to it.

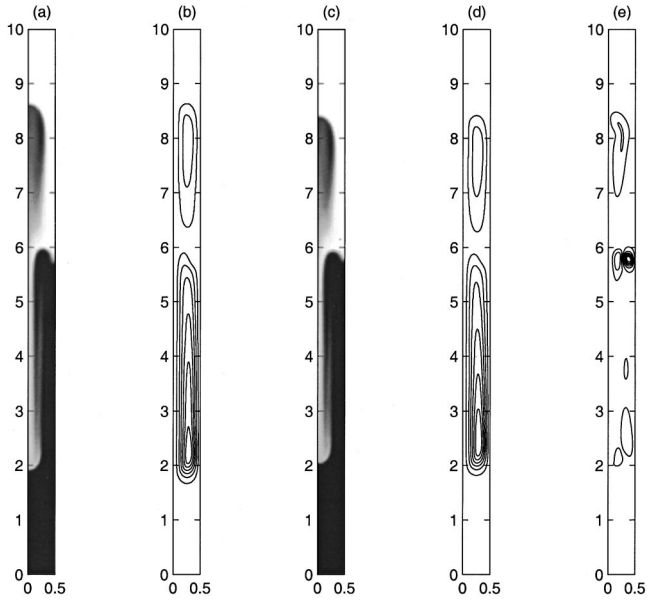

FIG. 9. Unstable evolution of the axisymmetric miscible interface. $\mathrm{Pe}=10^5$ and $R=-2.5$. (a) and (b) show the concentration and stream-function distributions in the absence of Korteweg stresses, while (c) and (d) present the corresponding information if the effects of Korteweg stresses are incorporated with $\delta=-10^{-4}$. For this case, (e) displays the component of the stream function that is due to the Korteweg stresses alone. Near the bubble tip, these stresses are seen to generate a ring-like structure that induces a downward velocity along the tube center, thereby slowing the bubble down.

3. Effects of nonvanishing divergence

In order to assess the influence of the divergence term generated in the mass-averaged velocity field by the density difference between the fluids, we carried out simulations for a range of ξ values, with $\mathrm{Pe}=10^5$ and $R=-2.5$, and in the absence of Korteweg stresses. Figure 10 presents the tip velocity data as a function of ξ. It is evident that for the present range of parameters the influence of the density difference on the quasisteady tip velocity V_{tip} is negligible. This is true even for fairly large values of up to $\xi=0.25$. Furthermore, the detailed distribution of the concentration field also looks quite similar with and without divergence effects, so that, at least for the current flow, this effect does not appear to be very influential.

IV. CONCLUSIONS

The present investigation addresses the question as to whether Korteweg stresses and/or divergence effects could potentially be responsible for discrepancies observed between Stokes flow simulations and experiments for miscible flows in capillary tubes. Conventional Stokes flow simulations that do not account for these effects show the emergence of quasisteady fingers for Pe values that are an order of magnitude smaller than the corresponding experimental values. We present an estimate of the effects of Korteweg stresses, and of the vorticity and stream-function fields induced by them, for net flow displacements in horizontal capillary tubes and density driven instabilities in vertical tubes. For both of these cases, the Korteweg stresses are seen to result in the formation of a vortex ring-like structure near the tip of the concentration front. Based upon the finding by Hu and Joseph[8] that the Korteweg stress coefficient has to be negative, we find that in the horizontal tube this vortex ring slows down the propagating front, which indicates that these

stresses can potentially account for the observed discrepancies mentioned above. In a similar fashion, in the vertical tube the Korteweg stresses are seen to slow down the rise of bubbles and fingers that evolve as a result of the unstable density stratification. Due to the unknown magnitude of the corresponding stress coefficients, more detailed quantitative comparisons are not possible at the present time.

Divergence effects are seen to be very small, and they have a negligible influence on the tip velocity. As a result, we can conclude that they are not responsible for the discrepancies between experiments and conventional Stokes simulations.

ACKNOWLEDGMENTS

The authors would like to thank Professor Tony Maxworthy and Dr. Philippe Petitjeans for helpful discussions. C.-Y. Chen was supported by ROC NSC (Grant No. NSC 89-2212-E-212-020). Furthermore, support was received from the NSF/ITR and NASA Microgravity programs, from Department of Energy–Basic Energy Sciences, and from Chevron Petroleum Technology Company, as well as through an NSF equipment grant.

[1]C.-Y. Chen and E. Meiburg, ''Miscible displacements in capillary tubes. Part 2: Numerical simulations,'' J. Fluid Mech. **326**, 57 (1996).
[2]P. Petitjeans and T. Maxworthy, ''Miscible displacements in capillary tubes. Part 1: Experiments,'' J. Fluid Mech. **326**, 37 (1996).
[3]G. I. Taylor, ''Deposition of a viscous fluid on the wall of a tube,'' J. Fluid Mech. **10**, 161 (1961).
[4]B. G. Cox, ''On driving a viscous fluid out of a tube,'' J. Fluid Mech. **14**, 81 (1962).
[5]D. A. Reinelt and P. G. Saffman, ''The penetration of a finger into a viscous fluid in a channel and tube,'' SIAM (Soc. Ind. Appl. Math.) J. Sci. Stat. Comput. **6**, 542 (1985).
[6]F. B. Bretherton, ''The motion of long bubbles in tubes,'' J. Fluid Mech. **10**, 166 (1961).
[7]G. I. Taylor, ''Dispersion of soluble matter in solvent flowing slowly through a tube,'' Proc. R. Soc. London, Ser. A **219**, 186 (1953).
[8]H. Hu and D. Joseph, ''Miscible displacement in a Hele-Shaw cell,'' Z. Angew. Math. Phys. **43**, 626 (1992).
[9]H. Davis, ''A theory of tension at a miscible displacement front,'' *Numerical Simulation in Oil Recovery*, IMA Volumes in Mathematics and Its Applications 11 (Springer, New York, 1988).
[10]D. Joseph and Y. Renardy, *Fundamentals of Two-Fluid Dynamics, Part II* (Springer, New York, 1992).
[11]C.-Y. Chen, L. Wang, and E. Meiburg, ''Miscible droplets in a porous medium and the effect of Korteweg stresses,'' Phys. Fluids **13**, 2447 (2001).
[12]D. Korteweg, ''Sur la forme que prennent les équations du mouvement des fluides si l'on tient compte des forces capillaires causées par des variations de densité,'' Arch. Neel. Sci. Ex. Nat. (II) **6**, 1 (1901).
[13]G. Galdi, D. Joseph, L. Prezisi, and S. Rionero, ''Mathematical problems for miscible, incompressible fluids with Korteweg stresses,'' Eur. J. Mech. B/Fluids **10**, 253 (1991).
[14]D. Joseph, A. Huang, and H. Hu, ''Non-solenoidal velocity effects and Korteweg stresses in simple mixture of incompressible liquids,'' Physica D **97**, 104 (1996).
[15]P. Petitjeans, ''Une tension de surface pour les fluides miscibles,'' C. R. Acad. Sci., Ser. IIb: Mec., Phys., Chim., Astron. **322**, 673 (1996).
[16]P. Petitjeans and P. Kurowski, ''Fluides non miscibles/fluides miscibles: des similitudes interessantes,'' C. R. Acad. Sci., Ser. IIb: Mec., Phys., Chim., Astron. **325**, 587 (1997).
[17]P. Kurowski and C. Misbah, ''A non-standard effect of diffusion on a fictitious front between miscible fluids,'' Europhys. Lett. **29**, 309 (1994).
[18]G. M. Homsy, ''Viscous fingering in porous media,'' Annu. Rev. Fluid Mech. **19**, 271 (1987).
[19]J. Fernandez, P. Kurowski, P. Petitjeans, and E. Meiburg, ''Density-driven, unstable flows of miscible fluids in a Hele-Shaw cell,'' J. Fluid Mech. **451**, 239 (2002).
[20]F. Graf, E. Meiburg, and C. Härtel, ''Density-driven instabilities of miscible fluids in a Hele-Shaw cell: Linear stability analysis of the three-dimensional Stokes equations,'' J. Fluid Mech. **451**, 261 (2002).
[21]D. Joseph, ''Fluid dynamics of two miscible liquids with diffusion and gradient stresses,'' Eur. J. Mech. B/Fluids **9**, 565 (1990).
[22]C. A. J. Fletcher, *Computational Techniques for Fluid Dynamics* (Springer, New York, 1988), Vol. 1.
[23]C.-Y. Chen, E. Meiburg, and L. Wang, ''The dynamics of miscible interfaces and the effects of Korteweg stresses,'' Trans. Aero. Astro. Soc. R.O.C. **33**, 7 (2001).
[24]R. Clift, J. R. Grace, and M. E. Weber, *Bubbles, Drops and Particles* (Academic, New York, 1978).